



# Aerosol-assisted CVD of cadmium diselenoimidodiphosphinate and formation of a new ${}^i\text{Pr}_2\text{N}_2\text{P}_3^+$ ion supported by combined DFT and mass spectrometric studies

Received 00th January 20xx,  
Accepted 00th January 20xx

DOI: 10.1039/x0xx00000x

www.rsc.org/

Temidayo Oyetunde,<sup>a</sup> Mohammad Afzaal,<sup>b</sup> Mark A. Vincent,<sup>c</sup> and Paul O'Brien<sup>\*d</sup>

Aerosol-assisted chemical vapour deposition (AACVD) of  $\text{Cd}[(\text{SeP}^i\text{Pr}_2)_2\text{N}]_2$  is shown to deposit cadmium selenide and/or cadmium phosphide on glass substrates, dependent upon the growth conditions. The phase, structure, morphology and composition of the films were characterised by X-ray powder diffraction (XRD), scanning electron microscopy, energy dispersive X-ray analysis and X-ray photoelectron spectroscopy. The XRD indicated an hexagonal phase for cadmium selenide, whilst cadmium phosphide was monoclinic. Pyrolysis gas chromatography-mass spectrometer and density functional theory were used to deduce a breakdown mechanism for the deposition that favoured the formation of a new aromatic  ${}^i\text{Pr}_2\text{N}_2\text{P}_3^+$  ion.

## Introduction

Coordination compounds containing direct metal and chalcogenide bonds have been extensively investigated by our group due to their ability to serve as efficient single-source precursors for chemical vapor deposition (CVD) of thin films or nanocrystals<sup>1-3</sup>. Good precursors for example, dithio- or diseleno-carbamates must meet a number of requirements including: high purity, exclusion of extrinsic impurities that can act as dopants and clean decomposition on the substrate surface.<sup>3</sup> The dichalcogenido imidodiphosphinate ligands,  $[(\text{EPR}_2)_2\text{N}]^-$  (E = S, Se, Te) considered as inorganic analogues of acetylacetonates display rich coordination behaviour towards main group and transition metal ions<sup>4-11</sup>. Thin films have been prepared from these at reduced or atmospheric pressure involving delivery at low pressure, from an aerosol or by entrainment<sup>12-14</sup>. Cadmium chalcogenide thin films or nanoparticles have been deposited from single-source precursors<sup>15</sup>. In our previous investigations on a series of nickel compounds  $\text{Ni}[{}^i\text{Pr}_2\text{P}(\text{E})\text{NP}(\text{E}'){}^i\text{Pr}_2]_2$  (E, E' = S; E, E' = Se; E = S, E' = Se), nickel sulfide, selenide or phosphide thin films

were generated; the material deposited depended on both temperature and the method used for the deposition<sup>16,17</sup>. We discovered that if the precursor has substantial residence time in the CVD reactor, it allows the generation of  $\text{PNP}^+$  ions leading to the formation of thermodynamically stable metal phosphide. To support the growth observations, pyrolysis gas chromatography mass spectrometry (Py-GC/MS) and density functional theory (DFT) studies were carried out to deduce the breakdown mechanism for the precursor.

The AACVD of  $\text{Cd}[(\text{SP}^i\text{Pr}_2)_2\text{N}]_2$  resulted in the deposition of cadmium sulfide and/or phosphide thin films<sup>18</sup>. We attempted to develop an understanding of the processes which led to different materials being deposited at different growth conditions. The GC-MS results coupled with DFT calculations indicated a plethora of pathways which could easily switch reactions over a short range of temperature. Hence, this resulted either in direct deposition or metathesis to the phosphide. Herein, we report the deposition of cadmium selenide and cadmium phosphide films from the AACVD of  $\text{Cd}[(\text{SeP}^i\text{Pr}_2)_2\text{N}]_2$ , which contains selenium ions as chalcogenide donor atoms. In addition, a new aromatic ion was identified in the mass spectrum based on the DFT explanation. As a semiconductor, cadmium selenide has n-type conductivity with a band gap of 1.74 eV<sup>19</sup>. The photosensitivity of cadmium selenide is responsible for its application in the production of optoelectronic devices such as photo electrochemical (PEC) cells<sup>20,21</sup>, photoconductors, thin film transistors and gamma ray detectors etc<sup>22,23</sup>. Cadmium phosphide is an n-type semiconductor with a band gap of  $\sim 1.2$  eV<sup>24</sup> which can be used in optoelectronics<sup>25</sup>, quantum electronics<sup>26</sup> and shows promise for thermo photovoltaic devices<sup>27</sup>. In addition, we have used Py-GC/MS

<sup>a</sup> Department of Chemical Sciences, College of Natural Sciences, Redeemer's University, Ede, Osun State. Nigeria

<sup>b</sup> Materials and Physics Research Centre, University of Salford, Salford, M54WT, United Kingdom

<sup>c</sup> School of Chemistry, The University of Manchester, Oxford Road, Manchester, M13 9PL, United Kingdom

<sup>d</sup> School of Chemistry and School of Materials, The University of Manchester, Oxford Road, Manchester, M13 9PL, United Kingdom. E-mail: Paul.O'Brien@manchester.ac.uk

† Footnotes relating to the title and/or authors should appear here.

Electronic Supplementary Information (ESI) available: Thermogravimetric analysis, X-ray photoelectron spectra and pyrolysis gas chromatography mass spectrum and density functional theory calculations.

See DOI: 10.1039/x0xx00000x

and DFT to explain the observed trends. Under low-pressure (LP) CVD studies, the same complex exclusively deposited cadmium selenide thin films at all deposition parameters<sup>8,28,29</sup>. It is worth recalling that the precursor purity is essential to avoid incorporation of extraneous elements, especially those that are electrically active. These can arise during the precursor synthesis or be incorporated into the material from the decomposition of the precursor (*e.g.*, carbon from an alkyl group).

### Experimental

All synthetic procedures were carried out under an inert atmosphere using a double manifold Schlenk-line, attached to an Edwards E2M8 vacuum pump, and a dry nitrogen cylinder. Chemicals were purchased from Sigma-Aldrich and Fischer Chemicals and were used as received. Dry solvents were used throughout the syntheses, either distilled over standard drying agents (Na/benzophenone, CaH<sub>2</sub> etc.) or purchased and stored in flasks over molecular sieves. Elemental analyses were performed by the microanalysis section of the School of Chemistry, University of Manchester. Thermogravimetric analysis (TGA) measurements were performed using Seiko SSC5200/S220TG/DTA model with a heating rate of 10 °C min<sup>-1</sup> under nitrogen. NMR spectra were recorded using a Bruker Avance (III) 400 MHz FT-NMR spectrometer, using CDCl<sub>3</sub> or *d*<sub>8</sub>-toluene as solvent. <sup>1</sup>H NMR spectra were referenced to the solvent signal and the chemical shifts were reported relative to Me<sub>4</sub>Si. <sup>31</sup>P NMR spectra were referenced externally to an 85% solution of H<sub>3</sub>PO<sub>4</sub> and the chemical shifts were reported relative to H<sub>3</sub>PO<sub>4</sub>. For pyrolysis GC-MS, small quantities of precursors were dissolved in dichloromethane, 5 µl was inserted in pyrolysis tubes dried at 80 °C and analysed by normal flash pyrolysis gas chromatography mass spectrometry (Py-GC-MS). Samples were pyrolysed using a CDS 5200 series pyroprobe pyrolysis unit by heating at 300 °C for 10 seconds. The fragments obtained were analysed using a Agilent 7890A linked to an Agilent 5975 MSD single quadrupole MS operated in electron ionisation (EI) mode (scanning between 50 and 800 atomic mass unit at 2.7 scans s<sup>-1</sup>; ionisation energy 40 eV). The chromatography conditions were as follows: HP5 fused column (J+W Scientific); bonded phase 5% diphenyldimethylpolyolsiloxane, length 30 m, inner diameter 0.32 mm; film thickness 0.25 mm. The temperature employed for analysis was: initial temperature 40 °C for 2 minutes, followed by heating at 8 °C min<sup>-1</sup> to 300 °C. The pyrolysis transfer line and injector temperatures were set at 350 °C, the heated interface at 280 °C, the EI source at 230 °C and the MS quadrupole at 150 °C. The carrier gas (helium) pressure was kept at 14 psi with flow rate of 1 cm<sup>3</sup> min<sup>-1</sup> and the samples were introduced in split mode (split ratio 50:1).

### Synthesis of [Pr<sub>2</sub>P(Se)NHP(Se)Pr<sub>2</sub>]<sup>30</sup>

A solution of chlorodiisopropylphosphine (25 g, 164 mmol) in toluene (50 ml) was added dropwise to a solution of 1, 1, 1, 3, 3, 3-hexamethyldisilazane (13.2 g, 82 mmol) in hot toluene (50 ml) over 30 minutes. Heating at 90 °C and stirring was continued for 3 hours after which reaction was cooled to room temperature and selenium powder (12.53 g, 16 mmol) was

added. The mixture was further refluxed for 6 hours which turned orange, cooled to 0 °C and left overnight. This was concentrated under vacuum and washed with diethyl ether and cold toluene which gave a white crystalline powder. Yield: 9.5 g (30 %). Elemental analysis: Calculated for C<sub>12</sub>H<sub>29</sub>NP<sub>2</sub>Se<sub>2</sub>: C, 35.37; H, 7.18; N, 3.44; P, 15.22%. Found: C, 35.36; H, 7.15; N, 3.38; P, 15.34 %. <sup>1</sup>NMR, (δ, CDCl<sub>3</sub>, 400 MHz): δ = 1.34 (m, 24H, 8xCH(CH<sub>3</sub>)<sub>2</sub>); 2.70 (m, 4H, 4xCH(CH<sub>3</sub>)<sub>2</sub>); 3.10 (s, 1H, -NH). <sup>31</sup>P{<sup>1</sup>H} NMR: 90.05 ppm. <sup>1</sup>J<sub>P-Se</sub> = 751 Hz.

### Synthesis of Cd[(SeP<sup>i</sup>Pr<sub>2</sub>)<sub>2</sub>N]<sup>30</sup>

The imidodiselenodiphosphinato ligand (4.55 g, 11.18 mmol) was dissolved in dry MeOH, stirred for 30 minutes and NaOMe (0.60 g, 11.18 mmol) added. A brown colouration was observed, followed by gentle heating which became progressively darker and transparent. CdCl<sub>2</sub> (1.28 g, 5.59 mmol) was added and a cloudy white suspension was observed immediately. The reaction continued for 3 hours and produced a cloudy white suspension, which was filtered and the off-white residue dissolved in hot dichloromethane. The resulting solution was filtered to remove excess reactant followed by solvent removal under vacuum. A pink powder obtained. Yield: 4.0g (77 %). Elemental analysis calculated for C<sub>24</sub>H<sub>56</sub>N<sub>2</sub>P<sub>4</sub>Se<sub>4</sub>Cd: C, 31.15; H, 6.10; N, 3.03; P, 13.40; Cd, 12.16 %. Found: C, 31.09; H, 6.30; N, 2.95; P, 13.10; Cd, 12.07 %. <sup>31</sup>P{<sup>1</sup>H} NMR (CDCl<sub>3</sub>): 56.4 ppm. <sup>1</sup>J<sub>P-Se</sub> = 385 Hz.

### Deposition of Thin Films

In a typical deposition experiment, 200 mg of the precursor was dissolved in 20 ml of toluene in a two-necked 100 ml round-bottom flask with a gas inlet which allowed the carrier gas (argon) to pass into the solution to aid the transport of the aerosol. The flask was connected to the reactor tube by a piece of reinforced tubing. For the deposition, the flow rate of the carrier gas was 160 or 240 sccm and was controlled by a Platon flow gauge. Seven glass substrates (*ca.* 1 x 3 cm) were placed inside the reactor tube, which was placed in a Carbolite furnace. The precursor solution in the round-bottom flask was kept in a water bath above the piezoelectric modulator of a PIFCO ultrasonic humidifier (Model No. 1077). The generated aerosol droplets of the precursor were transferred into the hot wall deposition zone of the reactor by the carrier gas. Both the solvent and the precursor were evaporated and the precursor vapour reached the heated substrate surface where thermally induced reactions and film deposition occurred.

### Characterisation of Thin Films

X-ray diffraction studies were performed on a Bruker AXS D8 diffractometer using monochromated Cu-Kα radiation. The samples were mounted flat and scanned from 10 to 80° in a step size of 0.05 with a count rate of 9 seconds. The diffraction patterns were then compared to the documented patterns in the ICDD index. All deposits were coated with carbon to avoid charging of the sample by the electron beam, using Edward's coating system E306A before scanning electron microscopy (SEM) was carried out. SEM was performed using a Philips XL30 FEG SEM. Energy dispersive X-ray (EDX) analyses were done using DX4 instrument. The XPS spectra were recorded using a Kratos Axis Ultra spectrometer employing a

monochromated Al  $K_{\alpha}$  X-ray source and an analyser pass energy of 80 eV (wide scans) or 20 eV (narrow scans) resulting in a total energy resolution of *ca.* 1.2 and 0.6 eV, respectively. Uniform charge neutralisation of the photoemitting surface was achieved by exposing the surface to low energy electrons in a magnetic immersion lens system (Kratos Ltd). The system base pressure was  $5 \times 10^{-10}$  mBar. Spectra were analysed by first subtracting a Shirley background and then obtaining accurate peak positions by fitting peaks using a mixed Gaussian/Lorentzian (30/70) line shape. During fitting, spin orbit split components were constrained to have identical line width, elemental spin orbit energy separations and theoretical spin orbital area ratios. Quantitative analysis was achieved using theoretical Scofield elemental sensitivities and recorded spectrometer transmission functions. All photoelectron binding energies (BE) were referenced to C1s adventitious contamination peaks set at 285 eV BE. The analyser was calibrated using elemental references; Au 4f<sub>7/2</sub> (83.98 eV BE), Ag 3d<sub>5/2</sub> (368.26 eV BE) and Cu 2p<sub>3/2</sub> (932.67 eV BE).

### Computational Studies

To model the breakdown of  $\text{Cd}(\text{SeP}(\text{R}_2)\text{-N-P}(\text{R}_2)\text{Se})_2$  ( $\text{R} = \text{iso-propyl}$ ) the 6-311G\*\* and SDD (Cd) basis sets were employed, together with the M06<sup>31</sup> functional, as implemented in the Gaussian09 suite of programs<sup>32</sup>. Free energies were determined using the harmonic oscillator and rigid rotor approximations at 1 atmospheric pressure and at 298.15 K and in some cases at 800 K.

### Results and Discussion

The purity of compound was confirmed by the NMR and elemental analysis. As indicated by the TGA, the complex sublimes cleanly (between 293 – 390 °C) with almost no residue (~2%), making it highly desirable for the CVD studies (Figure S1 in the Electronic Supporting Information, ESI).

AACVD studies were attempted on glass substrates at deposition temperatures between 475 and 525 °C, under dynamic argon flow rates of 160 or 240 sccm. The deposited black/grey thin films were found to be adherent but could be removed by scratching the film surfaces. Little or no film growth was seen at temperatures <450 °C. At 500 and 525 °C under an argon flow rate of 240 sccm, powder X-ray diffraction (XRD) analysis of the films confirmed hexagonal CdSe (ICDD 01-077-2307) (Figure 1a and b). In previous studies under LPCVD conditions, hexagonal cadmium selenide films were grown from  $[\text{Cd}\{(\text{SeP}^i\text{Pr}_2)_2\text{N}\}_2]^8$ ,  $[\text{Cd}\{(\text{SePPh}_2)_2\text{N}\}_2]^{28}$  and  $[\text{MeCd}\{(\text{SeP}^i\text{Pr}_2)_2\text{N}\}_2]^{29}$ . However, at the reduced flow rate of 160 sccm at 475 and 500 °C, heterogeneous films consisting of hexagonal CdSe (ICDD 01-077-2307) and monoclinic  $\text{Cd}_2\text{P}_3$  (ICDD 00-022-0125) were deposited. Traces of  $\text{Cd}_2\text{P}_3$  were more pronounced at 500 °C with  $2\theta$  values of 12.88, 27.08 and 29.06° (Figure 1c and d).

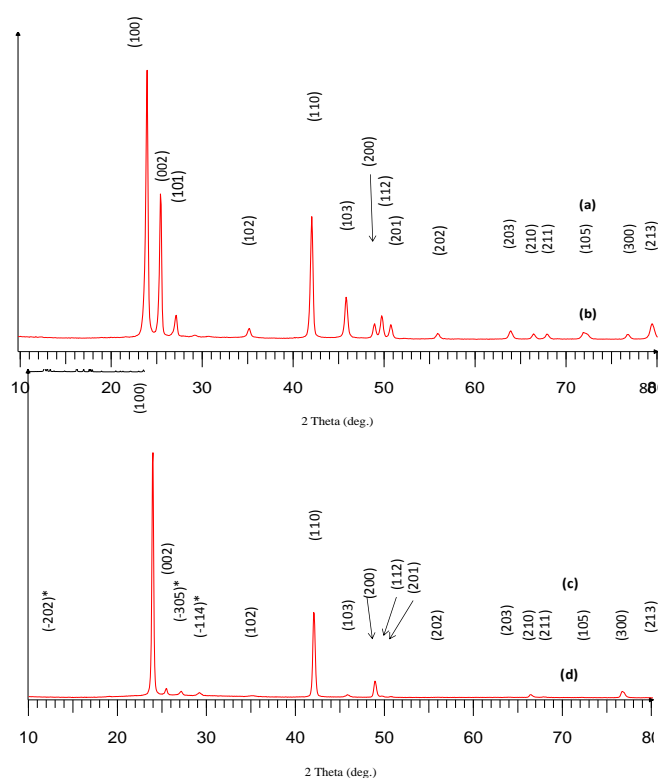


**Fig. 1** XRD pattern of deposited films at (a) 525 °C and (b) 500 °C, at flow rate of 240 sccm whereas (c) 500 °C and (d) 475 °C, at flow rate of 160 sccm. The marked peaks indicate the deposition of  $\text{Cd}_2\text{P}_3$ .

The scanning electron microscope (SEM) studies indicate that resulting morphologies are strongly temperature dependent. Interestingly, the films grown at 525 and 500 °C with an argon flow rate of 240 sccm had similar morphologies, and are comprised of randomly orientated fused platelets (Figure 2a and b). The surface morphology can be likened to previous CdSe films grown under LPCVD conditions from  $[\text{Cd}\{(\text{SeP}^i\text{Pr}_2)_2\text{N}\}_2]^8$ ,  $[\text{Cd}\{(\text{SePPh}_2)_2\text{N}\}_2]^{28}$  and  $[\text{MeCd}\{(\text{SeP}^i\text{Pr}_2)_2\text{N}\}_2]^{29}$ . However, the films deposited under exactly the same growth conditions but with a lower argon flow rate (160 sccm), consist of randomly orientated platelets (at 500 °C) and well aggregated and fused triangular crystallites (at 475 °C) (Figure 2c and d). The density of observed platelet-like morphology is higher at the increased flow rate but the thickness of platelets is somewhat greater at the lower flow rate. The energy dispersive X-ray analysis (EDAX) of hexagonal CdSe films showed cadmium-selenium ratio of ~1:1 together with *ca.* 10% phosphorus. For mixed CdSe and  $\text{Cd}_2\text{P}_3$  films, phosphorus content was increased to 26-29%. The cadmium to phosphorus ratio in the same film is greater than 1:1 whereas, for cadmium to selenium it is ~1:1.

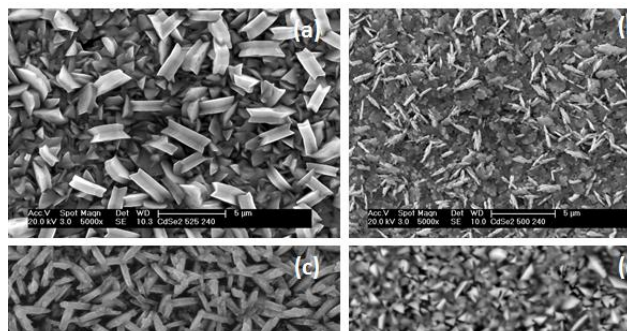


**Fig. 2** SEM images of deposited films at (a) 525 °C and (b) 500 °C, at flow rate of 240 sccm whereas (c) 500 °C and (d) 475 °C, at flow rate of 160 sccm.

The electronic structure of mixed CdSe and Cd<sub>2</sub>P<sub>3</sub> films, analyzed by X-ray photoelectron spectroscopy, (XPS) showed multiple species (Figures 3). The binding energies of Cd (3d<sub>5/2</sub> = 405.6, 3d<sub>3/2</sub> = 412.2 eV) and Se (3d<sub>5/2</sub> = 53.7, 3d<sub>3/2</sub> = 54.7 eV) peak positions indicate bulk CdSe<sup>33,34</sup>. The P 2p peaks are all around 134 eV BE and correspond to metaphosphate. The peak at 138.7 eV is due to Se LMM auger. The occurrence of the phosphide as phosphates might be due to the instability of the phosphide in air. Probably, they are more reactive (less stable) than the selenide and any surface phosphide which may be formed initially proceeded to form phosphate species as observed. The films used for XPS studies had been previously exposed to air during other measurements hence, significant oxidation of the surfaces might have occurred. Okamoto *et al.* reported that this value at 134 eV corresponds to a phosphate from an oxidized phosphorus<sup>35</sup>.

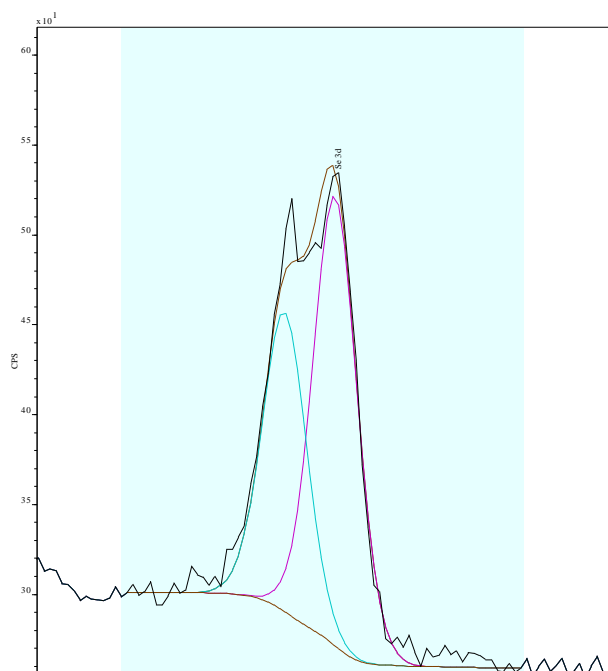


**Fig. 3** XPS of Se 3d (top), Cd 3d (middle) and P 2p (bottom) of deposited films.

#### Pyrolysis-GC/MS and DFT Studies of Cd[(SeP<sup>i</sup>Pr<sub>2</sub>)<sub>2</sub>N]<sub>2</sub>

Figure 4 shows the mass spectrum of the complex Cd[(SeP<sup>i</sup>Pr<sub>2</sub>)<sub>2</sub>N]<sub>2</sub> which is dominated by a peak with m/z 207 after 40 minutes. The exact nature of this peak is very interesting as no stable simple ion from the decomposition

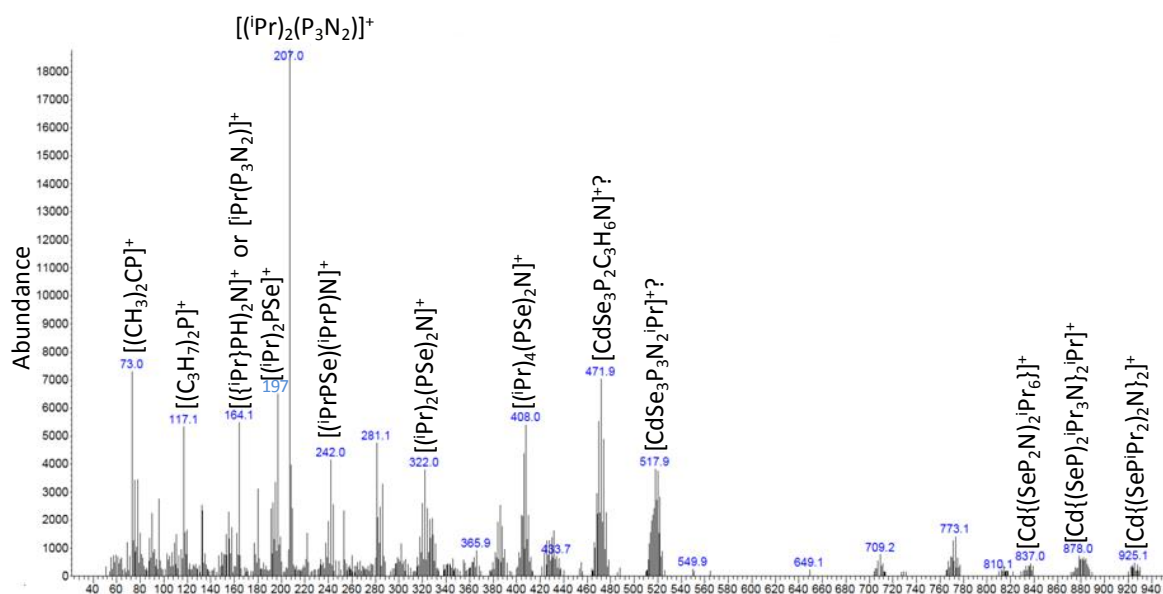


Fig. 4 Pyrolysis gas chromatography mass spectrum of  $\text{Cd}[(\text{SeP}^i\text{Pr}_2)_2\text{N}]_2$ .

of the complex has a peak at  $m/z$  207. From Figure 4 it can be seen that this peak has no adjacent isotopic signatures and hence, it consists of C, H, N and P.

To understand the decomposition pattern of the complex and the reason for the peak at  $m/z$  207 in the spectrum, we studied the thermal breakdown of the complex employing DFT calculations. Firstly, we investigated the parent ion ( $\text{Cd}(\text{SeP}(\text{R}_2)\text{-N-P}(\text{R}_2)\text{Se})_2^+$ ) and three possible breakdown paths: loss of R, loss of the entire neutral ligand and loss of the entire charged ligand. Respectively, the energetic values of these breakdown pathways are 126, 122 and 152  $\text{kJ mol}^{-1}$  (Figure S2). Once an entire ligand has been lost, the loss of the second (entire) ligand is a low energy process of 46 and 77  $\text{kJ mol}^{-1}$ . These sequences produce the same products containing two ligands: one charged and one neutral, and a Cd atom. The overall energetics of these two processes is  $\sim 198 \text{ kJ mol}^{-1}$ . Figures S3 and S4 give the breakdown of these ligands. The charged ligand cyclizes to an ion whose decomposition is energetic, as all the atoms in it exist in well-known stable valence states. It decays by the loss of an *iso*-propyl group and then another one from the same P atom (Figure S4). At this point it may lose  $\text{Se}_2$  to yield the ion  $\text{PNPR}_2^+$ . However, it costs exactly the same energy to form  $\text{RPNPR}^+$ , although the energetic parts of the path occur at different places (figure S4). Given that Figures S3 and S4 show various products that can be formed, which of these would give a peak at  $m/z$  207? It is clear that the peak at  $m/z$  207 arises from a very stable species as it still exists after 40 minutes. This rules out quite a few possible species and leaves the most likely candidate as  $\text{R}_2\text{N}_2\text{P}_3^+$ . This species is shown in Figure 5 along with other possibilities which would seem to be less stable. How is this specie, observed at  $m/z$  207, formed? Figure S2 gives the energetics to break off the

most likely candidate as  $\text{R}_2\text{N}_2\text{P}_3^+$ . This species is shown in ligands from the complex, while Figures S3 and S4 give the breakdown of the ligands. One sees that  $\text{R}_2\text{PNP}^+$  is as readily formed as NP. These react without barrier to form a linear ion  $\text{R}_2\text{PNPNP}^+$  which cyclizes readily (barrier: 26.0  $\text{kJ mol}^{-1}$  at 298.15 K). Theoretical calculations indicate that this isomer, with both *iso*-propyl groups on a single P atom, is not the most stable form and the lowest energy isomer has the *iso*-propyl groups bonded to the two nitrogen atoms. Additional computations on the parent system  $\text{H}_2\text{N}_2\text{P}_3^+$  show that this is more stable than  $\text{N}_2$  and  $\text{H}_2\text{P}_3^+$  by over 100  $\text{kJ mol}^{-1}$  (at 298.15 K). This indicates the stability of the ion in that one of the most stable molecules known ( $\text{N}_2$ ) does not possess sufficient energy to give a global minimum on the potential energy surface. Although our breakdown paths give the *iso*-propyl groups on phosphorus (Figures S2–S4), however, we have studied if these groups can rearrange to the more stable isomer in which they are bonded to the nitrogen atoms. Thus under the energetic conditions in which the mass spectrum is obtained, are the *iso*-propyl groups likely to move to give the most stable isomer? Consequently, we have modelled the movement of the *iso*-propyl moieties of  $\text{R}_2\text{N}_2\text{P}_3^+$  from being bound to one or two P atoms to that of being bonded to both nitrogen atoms. The energetics of this rearrangement depend on the exact species undergoing reaction, but the highest energy for the transfer occurred at 174.1  $\text{kJ mol}^{-1}$  at 298.15 K (167.6  $\text{kJ}$  at 800 K). This was from a cyclic species with both *iso*-propyl groups on the same phosphorus. The subsequent R group transfer happened at a lower energy of 86.2  $\text{kJ mol}^{-1}$  at 298.15 K (or 87.6  $\text{kJ mol}^{-1}$  at 800.0 K). These energies are not too dissimilar from those presented in Figures S2–S4. In addition, we note that in support for our suggested species (Figure 5A), a related ion has been prepared ( $\text{P}_2\text{N}_3^-$ )<sup>36</sup>,

although this has three nitrogen and two phosphorus atoms and no iso-propyl cations attached.

Hence, we have suggested the ion given in Figure 2A as the species observed at  $m/z$  207 partly because it is a stable aromatic species. To confirm its aromaticity, we determined the NICS<sup>37</sup> values of the parent ion ( $H_2N_2P_3^+$ ) and found a value of 14.2 compared to the corresponding benzene value of 10.2<sup>37</sup> at the B3LYP/6-311+G\*\* level of theory. This calculation confirms the aromaticity of this specie. While the major peak in the mass spectrum is at  $m/z$  207, there are several other moderate strength peaks that need to be assigned (Figure 4). The peak at  $m/z$  73 is  $(CH_3)_2C=P^+$ , which could perhaps rearrange to the triple bonded species  $CH_3CPCH_3^+$ . The peak at  $m/z$  117 is likely to be  $(C_3H_7)_2P^+$ , which like the peak at  $m/z$  73 might rearrange in this case to  $(CH_3)_2C=P(H)(C_3H_7)^+$ . At  $m/z$  164 and  $m/z$  197 in the mass spectrum there are peaks that may well be  $(C_3H_7)(H)P-N=P(H)(C_3H_7)^+$  and  $(C_3H_7)_2P=Se^+$  respectively, with a P bearing the charge and thus being four valent. While our breakdown of the ligands and complex given in Figure S3-S5 give low energy pathways, however, the very energetic nature of mass spectrometry means that many other breakdown pathways can be taken. However, we note that the large mass ions are consistent with the loss of iso-propyl groups, just as we have modeled (Figure S2).

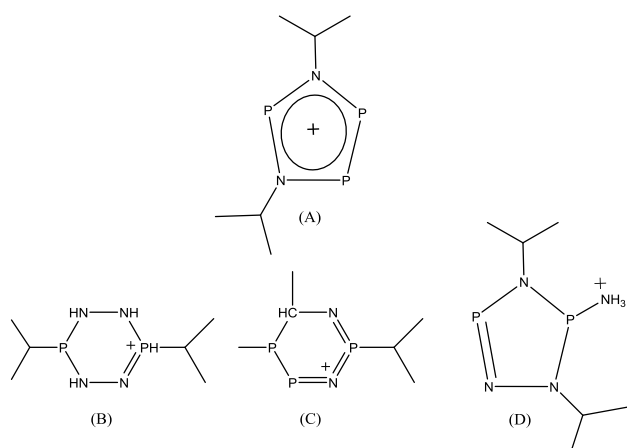


**Fig. 5** The suggested ion for the peak observed at 207 in the mass spectrum (A) and other possible but less likely ions (B-D).

The existence of a neutral form of the aromatic ion which we have postulated as the reason for the observed peak at  $m/z$  207 in the mass spectrum is unlikely, as it would not be aromatic. However,  ${}^iPr(P_3N_2)$  is a neutral aromatic species based on the  $P_3N_2$  aromatic ring system. Is it likely to occur in the CVD breakdown of  $Cd[(SeP^iPr_2)_2N]_2$ ? Our peak at  $m/z$  207 ( ${}^iPr_2N_2P_3^+$ ) in the mass spectrum can only refer to a charged species which is created by the ionizing conditions of a mass spectrometer. Consequently, the loss of an iso-propyl cation from this yields the neutral aromatic species  ${}^iPr(P_3N_2)$ . If it is formed in the vapour phase, a peak should be observed in the mass spectrum at  $m/z$  164 and indeed there is a peak at this charge to mass ratio, although it could refer to  $({}^iPrHP)_2N^+$ . Indeed, the breakdown of the neutral ligand occurs through

fragmentation as we observed for the ion  $Cd[(SeP^iPr_2)_2N]_2^+$  (Figures S3, S5 and S6). Consequently, the fragments which are necessary to form the neutral aromatic species would be available and thus, there is the possibility that the peak at  $m/z$  164 is due to this.

The calculations and the mass spectrum would indicate a variety of vapour phase species by which cadmium phosphide and selenide could be deposited. We have shown how  $P_2$  can be formed and NP (Figure S3), both of which could deposit with Cd to give  $Cd_xP_y$ .  $Se_2$  can also be formed and yield  $Cd_xSe_y$ . However, it is likely that some species having H or iso-propyl groups also were deposited but decomposed to give the CdPSe species observed.

## Conclusions

In conclusion, AACVD studies of  $Cd[(SeP^iPr_2)_2N]_2$  has shown that the material deposited depends largely on the growth conditions. Higher argon rates of 240 sccm result in the deposition of pure CdSe thin films, whereas lower flow rates (160 sccm) deposits a mixture of CdSe and  $Cd_2P_3$  films. The reason for the formation of CdSe/ $Cd_2P_3$  films is probed through a combination of DFT and pyrolysis GC-MS. The mass spectrum of the complex revealed a strong peak at  $m/z$  207, which we assigned to be a new aromatic specie. This ionic structure was based on theoretical calculations that indicate the most stable isomer contains the iso-propyl groups on nitrogen rather than phosphorus. In our future work, we shall investigate the AACVD of  $Cd[(SP^iPr_2)(SeP^iPr_2)_2N]_2$  precursor to ascertain the reproducibility of this result.

## Acknowledgements

T. O. acknowledges the School of Chemistry, University of Manchester for financial support. We thank Prof. I. Hillier for helpful discussions and for comments on the earlier versions of this manuscript. Also, the authors thank Dr. Paul Wincott for XPS measurements.

## References

- 1 A. N. Gleizes. *Chem. Vap. Dep.*, 2000, **6**, 155.
- 2 A. C. Jones, P. O'Brien. *CVD of Compound Semiconductors: Precursor Synthesis, Development and Applications*, VCH, Weinheim., 1997, ISBN: 3-527-29294-1.
- 3 (a) M. A. Malik, M. Afzaal, P. O'Brien. *Chem. Rev.*, 2010, **110**, 4417; (b) C. E. Knapp, C. J. Carmalt, *Chem. Soc. Rev.*, 2016, **45**, 1036.
- 4 (a) A. Schmidpeter, R. Bohm, H. Groeger. *Angew. Chem. Int. Ed. Engl.*, 1964, **3**, 704. (b) A. Schmidpeter, K. Stoll. *Angew. Chem. Int. Ed. Engl.*, 1967, **6**, 252. (c) A. Schmidpeter, K. Stoll. *Angew. Chem. Int. Ed. Engl.*, 1968, **7**, 549.
- 5 P. Bhattacharyya, A. M. Z. Slawin, D. J. Williams, J. D. Woollins. *J. Chem. Soc., Dalton Trans.*, 1995, 2489.
- 6 For a review, see: C. Silvestru, J. E. Drake. *Coord. Chem. Rev.*, 2001, **223**, 117.
- 7 For a review, see: T. Q. Ly, J. D. Woollins. *Polyhedron.*, 1998, **176**, 451.



- 8 M. Afzaal, D. Crouch, M. A. Malik, M. Motevalli, P. O'Brien, J. H. Park, J. D. Woollins. *Eur. J. Inorg. Chem.*, 2004, 171.
- 9 D. J. Crouch, P. O'Brien, M. A. Malik, P. J. Skabara, S. P. Wright. *Chem. Comm.*, **2003**, 1454.
- 10 M. Afzaal, D. J. Crouch, P. O'Brien, J. Raftery, P. J. Skabara, A. J. P. White, D. J. Williams, *J. Mater. Chem.*, 2004, **14**, 233.
- 11 D. Cupertino, D. J. Birdsall, A. M. Z. Slawin, J. D. Woollins. *Inorg. Chim. Acta.*, 1999, **290**, 1.
- 12 L. V. Interrante, M. J. Hampden-Smith. *Chemistry of Advanced Materials: An Overview*, Wiley-VCH., 1998, 176.
- 13 P. O'Brien. *Encyclopedia of Materials: Science & Technology*, Elsevier **2001**, 1173.
- 14 J. S. Ritch, T. Chivers, M. Afzaal, P. O'Brien.; *Chem. Soc. Rev.*, 2007, **36**, 1622.
- 15 (a) M. A. Malik, M. Afzaal, P. O'Brien.; *Chem. Rev.*, 2010, **110**, 4717. (b) M. Afzaal, M. A. Malik, P. O'Brien. *J. Mater. Chem.*, 2010, **20**, 4031.
- 16 A. Panneerselvam, G. Periyasamy, M. A. Malik, M. Afzaal, P. O'Brien, M. Helliwell. *J. Am. Chem. Soc.*, 2008, **130**, 2420.
- 17 A. Panneerselvam, G. Periyasamy, K. Ramasamy, M. Afzaal, M. A. Malik, P. O'Brien, N. A. Burton, J. Waters, B. E. Van Dongen. *Dalton Trans.*, 2010, **39**, 6080.
- 18 D. Oyetunde, M. Afzaal, M. A. Vincent, I. H. Hillier, P. O'Brien. *Inorg. Chem.*, 2011, **50**, 2052.
- 19 K. N. Shreekanthan, B. V. Raiendra, G. K. Shivakumar, *Cryst. Res. Technol.*, **38**, 2003, 30.
- 20 S. M. Pawar, A. V. Moholkar, C. H. Bhosale. *Mater. Lett.*, 2007, **61**, 1034.
- 21 X. Matthew, J. Pantoja Enriquez, A. Romeo, A. N. Tiwari.; *Solar Energy* 2004, **77**, 831.4
- 22 S. Utahna, P. J. Reddy. *Phys. Status Solidi*, 1981, **A65**, 269.
- 23 A. K. Rautri, R. Thangaraj, A. K. Sharma, B. B. Tripathi, O. P. Agnivotri. *Thin Solid Films*, 1982, **91**, 55.
- 24 I. E. Zanin, K. B. Aleinikova, M. Y. Antipin, M. M. Afanasiev. *J. Struct. Chem.*, 2006, **47**, 78.
- 25 I. T. Bodnar, V. M. Trukhan, A. U. Sheleg. *J. Opt. Tech.*, 2006, **73**, 525.
- 26 I. T. Bodnar, V. M. Trukhan, A. U. Sheleg. *J. Appl. Spec.*, 2006, **73**, 776.
- 27 A. M. Hermann, A. Madam, M. W. Wanlass, V. Badri, R. Ahrenkiel, S. Morrison, C. Gonzalez. *Sol. Ener. Mat. & Sol. Cells.*, 2004, **82**, 241.
- 28 M. Afzaal, S. M. Aucott, D. Crouch, J. D. Woollins, J. H. Park, P. O'Brien. *Chem. Vap. Dep.*, 2002, **8**, 187.
- 29 M. Afzaal, D. Crouch, M. A. Malik, M. Motevalli, J. H. Park, P. O'Brien. *J. Mater. Chem.*, 2003, **13**, 639.
- 30 D. Cupertino, D. J. Birdsall, A. M. Z. Slawin, J. D. Woollins. *Inorg. Chim. Acta.*, 1999, **290**, 1.
- 31 M. T. S. Nair, P. K. Nair. *J. Appl. Phys.*, 1993, **74**, 3, 1879.
- 32 Y. Zhan, D. G. Truhlar. *Theor. Chem. Acc.*, 2008, **120**, 215.
- 33 M. J. Frisch, G. W. Trucks, H. B. Schlegel, G. E. Scuseria, M. A. Robb, J. R. Cheeseman, G. Scalmani, V. Barone, B. Mennucci, G. A. Petersson, H. Nakatsuji, M. Caricato, X. Li, H. P. Hratchian, A. F. Izmaylov, J. Bloino, G. Zheng, J. L. Sonnenberg, M. Hada, M. Ehara, K. Toyota, R. Fukuda, J. Hasegawa, M. Ishida, T. Nakajima, Y. Honda, O. Kitao, H. Nakai, T. Vreven, J. A. Montgomery, Jr., J. E. Peralta, F. Ogliaro, M. Bearpark, J. J. Heyd, E. Brothers, K. N. Kudin, V. N. Staroverov, R. Kobayashi, J. Normand, K. Raghavachari, A. Rendell, J. C. Burant, S. S. Iyengar, J. Tomasi, M. Cossi, N. Rega, J. M. Millam, M. Klene, J. E. Knox, J. B. Cross, V. Bakken, C. Adamo, J. Jaramillo, R. Gomperts, R. E. Stratmann, O. Yazyev, A. J. Austin, R. Cammi, C. Pomelli, J. W. Ochterski, R. L. Martin, K. Morokuma, V. G. Zakrzewski, G. A. Voth, P. Salvador, J. J. Dannenberg, S. Dapprich, A. D. Daniels, Ö. Farkas, J. B. Foresman, J. V. Ortiz, J. Cioslowski, and D. J. Fox. *Gaussian 09, Revision A.01*, Gaussian, Inc., Wallingford CT, 2009.
- 34 J. E. B. Katari, V. L. Colvin, A. P. Alivisatos. *J. Phys. Chem.*, 1994, **98**, 4109.
- 35 Y. Okamoto, Y. Nitta, T. Imanaka, S. Teranishi, *J. Chem. Soc., Faraday Trans. 1.*, 1979, **75**, 2027.
- 36 A. Velain, C. C. Cummins, *Science*, 2015, **348**, 1001.
- 37 Z. Chen, C. S. Wannere, C. Corminboeuf, R. Puchta, P. v. R. Schleyer. *Chem. Rev.*, 2005, **105**, 3842.